The Effect of Sintering Temperature on Microstructure and Hardness of the Milled WC- 20 Wt.% Equiatomic (Fe,Co) Cemented Carbides

Mi. Karbasi[a,*], Ma. Karbasi[a], A. Saidi[a], M. H. Fathi[a]

[a] *Department of Materials Engineering, Isfahan University of Technology, Isfahan, Iran.*

ARTICLE INFO

Article history:

Received 23 April 2014
Accepted 01 January 2015
Available online 15 March 2015

Keywords:

Cemented carbides
Microstructure
Mechanical properties
Sintering temperature

ABSTRACT

In this study, WC–20 wt.% equiatomic (Fe,Co) powder mixture was milled in a planetary ball mill. The effects of different milling times (15 min, 5h, 10h, and 25 h) and sintering temperatures on the microstructure and mechanical properties of this equi-Fe substituted cermet were investigated. The structural evolution and the crystallite size changes of the powders during milling were monitored by X-ray diffraction (XRD). Microstructural developments of the samples were examined using scanning electron microscopy (SEM). The results showed that the crystalline size of WC and internal strain were 22 nm and about 1.1 % after 25 hours of milling, respectively. The hardness and the relative density of the WC-20wt.% (Fe,Co) composites, consolidated by conventional sintering at different temperatures, ranging from 1150 to 1450 ˚C in hundreds, were investigated. The optimized sintering temperature was specified at 1350°C. At a constant sintering temperature, 1350°C, the highest relative density of 98.2% and hardness of 1281 (HV30) were obtained for the milling time of 25h.

1. Introduction

Cemented carbides such as WC–Co have been used in various commercial and technological applications for the last decades due to the extreme hardness, high elastic modulus and flexural strength over the other materials. The great properties of the cemented tungsten carbides make them useful as cutting tools, rock drills, punches, extrusion, pressing dies, and wear-resistant coatings[1, 2].

Although the WC-Co composites are the most important commercial grade of WC cements, they have several disadvantages such as: the market price fluctuations, environmental toxicity of cobalt, poor resistance to oxidation at elevated temperature (i.e. above 600˚C), and corrosion problems [3, 4]. Therefore, significant research efforts have been made to replace cobalt by other transition metals of the VIII group, such as iron [5-7] or nickel [8-10], as a binding metal to overcome the shortcomings of the WC-Co composites.

Researches by Prakash [11] demonstrated that cemented carbides with Fe-rich binders enhanced properties such as higher hardness, abrasive wear resistance, toughness, and strength properties compared with the Co-bonded hard metals. Other researchers also reported similar and superior values for hardness, toughness, and transverse rupture strength (TRS) over the

Corresponding author:
E-mail address: M.Karbasi@ma.iut.ac.ir (Minoo Karbasi).

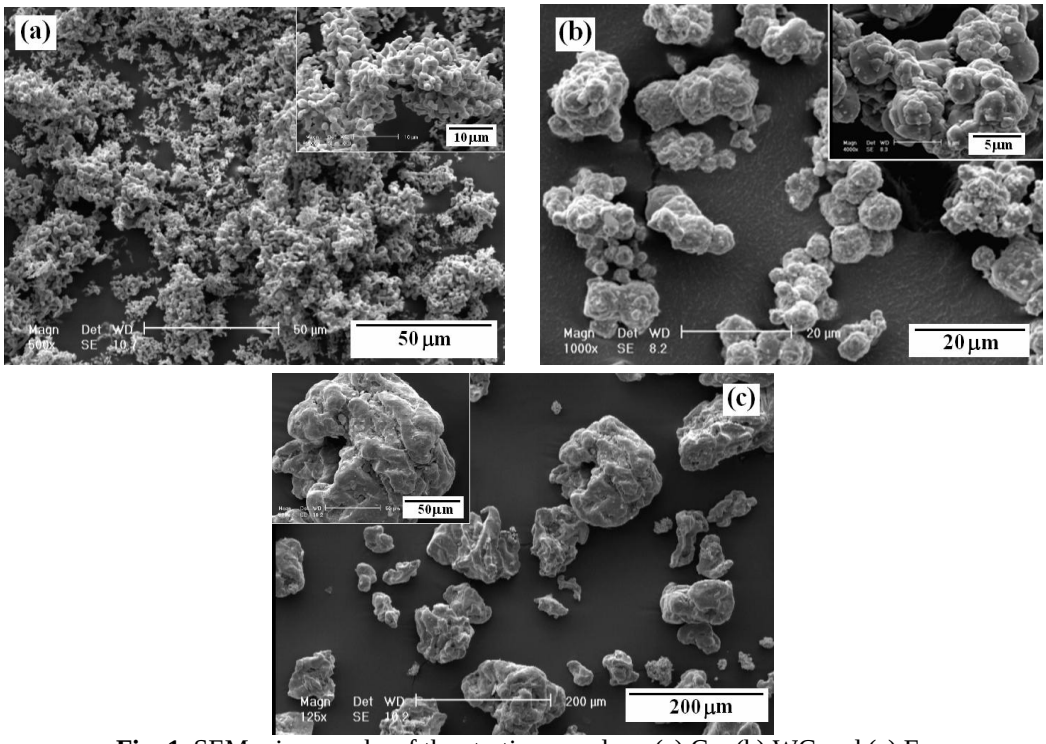

Fig. 1. SEM micrographs of the starting powders: (a) Co, (b) WC and (c) Fe

WC–Co system [5, 9, 12]. In the case of substitution of cobalt by nickel as a binder, Perter and Brabyn [13] showed that the maximum fracture toughness could be achieved by WC-7Co-3Ni.

General methods of synthesizing the nanostructured WC or WC–Co composite include spraying conversion process, co-precipitation, displacement reaction process, mechanochemical synthesis, and mechanical alloying (MA)[14]. Recently, MA process has become a popular method to fabricate nano crystalline materials due to its simplicity and relatively inexpensive equipment [15]. Cemented tungsten carbide with nano-crystalline grain structure has the potential to dramatically improve the mechanical properties of these materials [16]. In this research, WC–20 wt.% equiatomic (Fe,Co) was milled at different milling times. The sintering behavior of these powders and the influence of the sintering temperature on the hardness of the sintered samples was also investigated.

2. Experimental

2. 1. Starting materials

High purity (>99.5%, Merck) starting materials (WC, Co, Fe) were used for the preparation of the composites. The SEM micrographs of the starting powders are shown in Fig. 1.

2. 2. Composite preparation

Fe and Co powders with Fe/Co weight ratio of 1/1 with 80 wt. % WC were milled in a planetary ball mill under argon atmosphere at different milling times of 15 min, 5, 10 and 25 hours. The ball-to-powder weight ratio and the rotational speed were 20:1 and 500 rpm, respectively. Green bulk samples were prepared by cold-pressing of the powder mixtures in a cylindrical steel die. For all of the samples, the compaction pressure was 500 MPa.

2. 3. Sintering and characterization

Sintering was performed at different temperatures, ranging from 1150 to 1450 ˚C in hundreds, for 60 minutes under hydrogen atmosphere controlled by hydrogen generator (SHC-300). The heating rate was set to 10 $^{\circ}Cmin^{-1}$. The density of the sintered parts was determined by the water displacement (Archimedes) method. The samples for metallographic study were prepared according

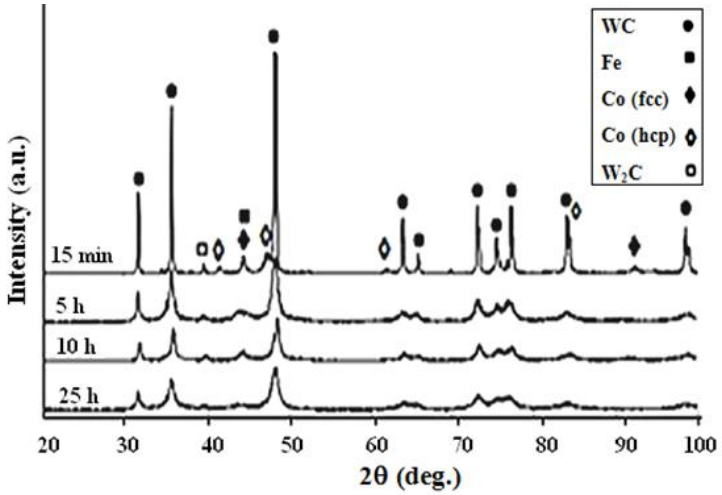

Fig. 2. X-ray diffraction of the WC-Fe-Co composite powder at several milling times

to the ASTM B665 standard. The structure of the samples was characterized by a Philips X'PERT MPD X-ray diffractometer with Cu-Kα radiation (λ=0.154056 nm). The crystallite size and internal strain of the powders were calculated from the broadening of the XRD peaks using the Williamson–Hall method [17].

$$B\cos\theta = 0.9\frac{\lambda}{D} + \varepsilon\sin\theta$$

Where B is the full-width at half maximum intensity, λ is the wavelength of the X-ray used, D is the average crystallite size, θ is the Bragg angle and ε is the average strain. Powder morphology and microstructure developments were examined using a Philips XL30 scanning electron microscope (SEM). Vickers hardness of the compacts was measured at a load of 293 N (HV30) and dwell time of 10 s.

3. Results and discussion

3. 1. Characterization of the milled WC-Fe-Co powder

The X-ray diffraction patterns of the powder mixture after different MA times are presented in Fig. 2. As can be seen, the starting powders contain Fe, Co, WC and small amounts of the W_2C phase. It is note-worthy that the Co phase is composed of the fcc (α) and hcp (ε) phases. The disappearance of the Co peaks after 5 hours of milling can be explained by dissolution of Co into Fe (the bcc structure) in order to form the (Fe-Co) solid solution, as shown elsewhere [18, 19]. Increasing the milling time is accompanied by line broadening and a steep decrease in the intensity due to the decrease of the grain size and increase of the internal strain as a result of milling.

The crystallite size and internal strain of the WC phase calculated from the line width were 22 nm and about 1.1 percent after 25 h milling. The reduction of the crystalline size during the milling process was because of the localization of plastic deformation (in the form of shear bands containing a high density of dislocations), formation of cells and sub-grains by annihilation of dislocations as well as the conversion of sub-grains into grains through mechanically driven grain rotation and sub-grain boundary sliding [20]. The SEM images in Fig. 3 show the changes in the microstructure of the composite powder with increase of the milling time.

In Fig. 3a, based on the EDS results, WC, Fe and Co particles are shown in white, light grey and dark grey colors, respectively. As can be seen, after milling for 15min, only a partially physical mixture was formed and the Fe, Co and WC powders had different particle distributions. After 5 hours of milling (Fig. 3b), particle size was reduced and better distributions of the components were observed. Phase distribution homogeneity was developed by further milling up to 10 hours (Fig. 3c). As can be seen in Fig. 3d, the particle size was reduced and all of the particles were completely homogenous. With the decrease of the fragment size, the tendency to aggregate increases,

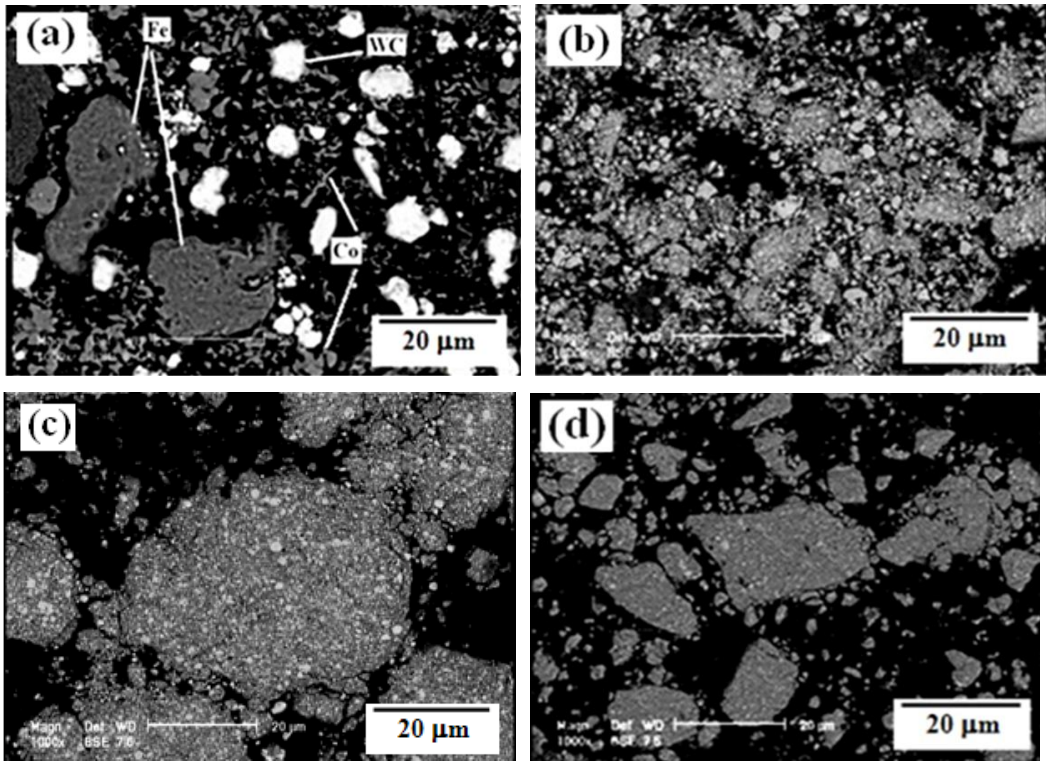

Fig. 3. The cross-sectional SEM micrographs of the WC-20 wt. %(Fe,Co) composite particles at different milling times: (a) 15 min, (b) 5h, (c)10h, (d) 25h

thereby causing the increase of fracture resistance. Particle fineness approaches a limit as milling continues and maximum energy is expended [18].

3. 2. Characterization of the sintered WC-Fe-Co composite

Homogenous distribution of WC in (Fe-Co) solid solution binder was achieved after 25 hours of milling. Consequently, the powder sample milled for 25 hours was compacted and sintered at different temperatures of 1150 to 1450˚C in hundreds. Fig. 4 shows the microstructure of the 25-hours-milled powders sintered at different sintering temperatures. It is evident that with the increase of sintering temperature, the initial relatively round WC grains become faceted. The grain growth of WC in cemented carbides generally occurs in two modes, namely, coalescence process and solution/reprecipitation process [21]. After sintering at 1150˚C, WC forms irregular morphology. At 1250˚C, the formation of anomalously large WC grains in the microstructure is because of the coalescence mechanism at this temperature. With the increase of temperature, the WC grains exhibit faceted morphology. Solution/reprecipitation increases as the temperature increases [22]. Furthermore, at high temperatures (1350˚C and 1450˚C) the Solution/reprecipitation structure becomes dominant: smaller grains dissolve because of their higher dissolution. On the other hand, the coarser ones grow by material re-precipitation and reduce the interface area of the system. So, rounded WC particles change into a faceted shape [12, 23-24]. The difference in the surface energy of the (0 1 0) and (1 0 0) planes leads to the formation of faceting structure. Because of this anisotropy, the WC grains tend to assume an equilibrium shape (truncated triangular prism (Fig. 5)), as observed elsewhere [23, 24].

The changes in relative density of the sintered composites after 25 hours of ball milling as a function of sintering temperature are shown in Fig. 6. It can be concluded that the relative density increases sharply at sintering temperature above 1150˚C up to 1450˚C, and reaches a saturated value at the sintering

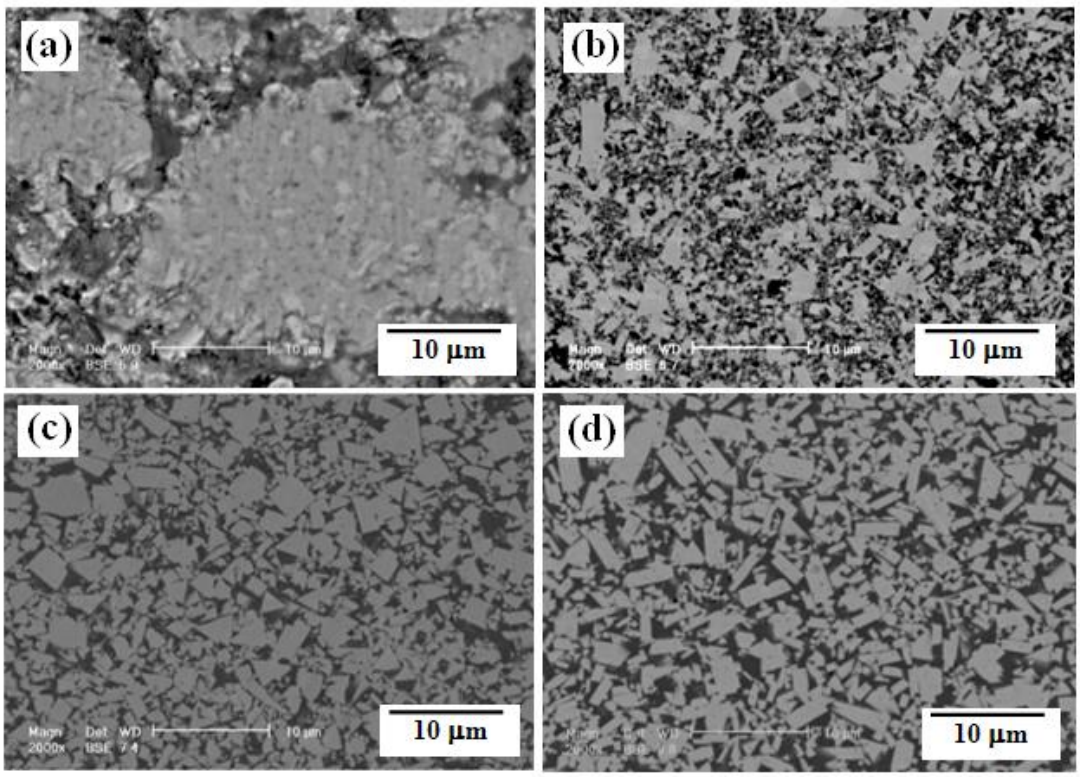

Fig. 4. SEM micrographs of the sintered samples prepared from powder ball milled for 25 hours as a function of the sintering temperature: a) 1150˚C, b) 1250˚C, c) 1350˚C and d) 1450˚C

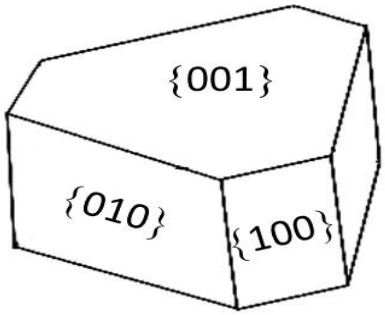

Fig. 5. Schematic of truncated trigonal prism (equilibrium shape of WC crystals) [23]

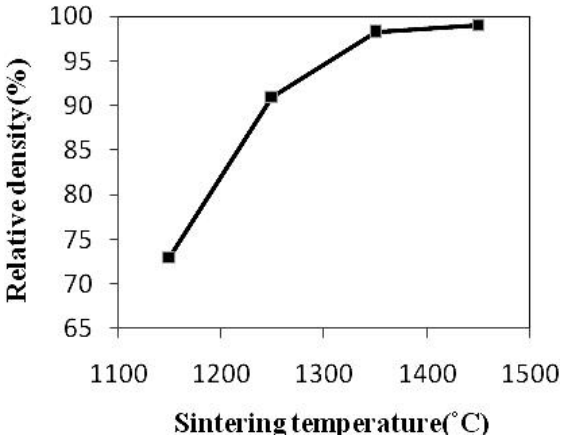

Fig. 6. Effect of the sintering temperature on the relative density of the sintered composite after 25 hours of ball milling

temperature of 1350˚C. As the temperature increases, porosities decrease due to the higher liquid phase transaction during sintering that could be a reason for increasing relative density [25, 26].

The effect of the sintering temperature on the hardness is shown in Fig. 7. Hardness has a rapid increasing behavior above 1250˚C, but it gradually grows below this temperature. Generally, hardness of the cemented carbides is affected by different parameters such as amount and type of the binder, size, distribution and the contiguity of the carbide phase, and porosity [27-29]. So, the rapid increase of

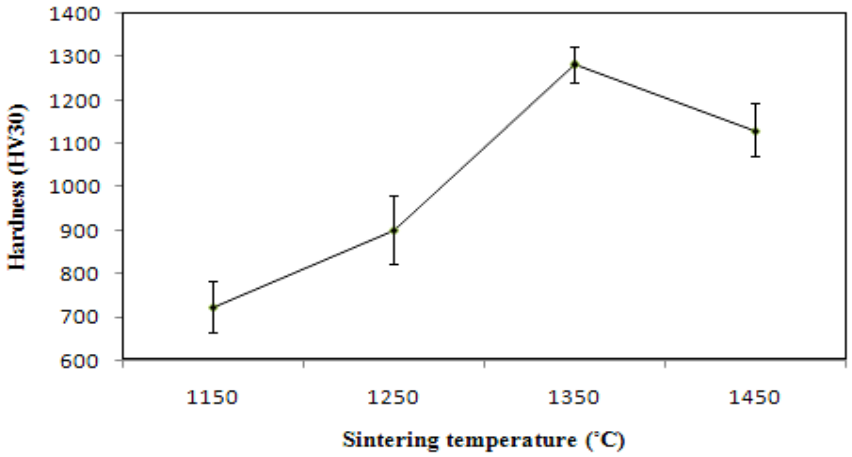

Fig. 7. Effect of the sintering temperature on hardness of the sintered composite after 25 hours of ball milling

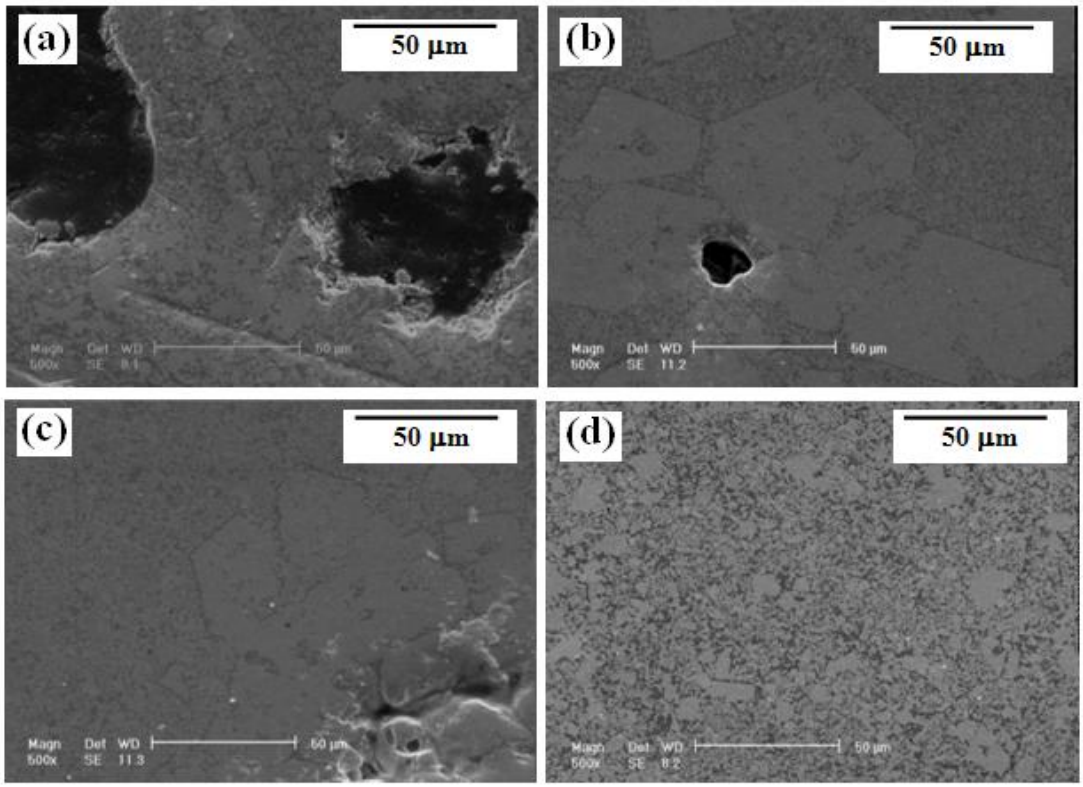

Fig. 8. The micrographs (SE mode) of sintered samples at 1350°C with various milling times

hardness above 1250˚C seems to occur due to the formation of a liquid phase during sintering which leads to sharply increase the relative density [23, 26]. Moreover, the hardness slightly decreases above 1350˚C. It can be attributed to the fact that the sintered density reaches the saturated value, but the crystallite size of WC considerably increases at temperatures above 1350˚C [30].

By considering the hardness and densitometry characterization results shown in Figs. 6 and 7, further sintering experiments were carried out at 1350°C as optimized sintering condition. Fig. 8 shows microstructure development of the sintered samples at 1350°C with various milling times.

The results show that the sintering behavior of the composite powder is significantly

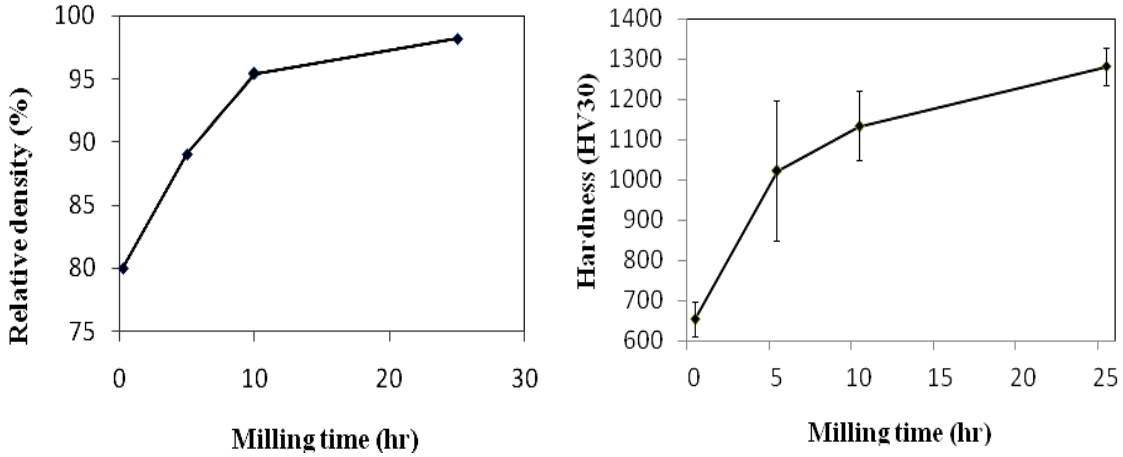

Fig. 9. Effects of the milling time on relative density and hardness of the milled powders sintered at 1350˚C temperature

influenced by ball milling. The most important finding is that sintering of the 15 minutes milled powder at 1350 ˚C resulted in a small densification. The binder does not have uniform distribution in the 15-minutes-milled sample and high porosity features are apparent in the SEM (secondary mode) micrograph. As can be seen in Fig. 8, increasing the milling time has important effects on distribution and densification: better distibution of binder and a progressive increment in the densification as well as reduction of porosities. The 25-hours-milled powder shows noticeable densification on liquid phase sintering. As a result of densification on the liquid phase, the density of the sample reaches to 98.2%TD. The effects of the milling time on relative density and hardness of the milled powders sintered at 1350˚C temperature are indicated in Fig. 9.

At a constant sintering temperature, a higher density is achieved at higher milling time. This observation is related to the effect of milling time on the microstructure of the composite powder. As shown elsewhere [1,33], the WC particles undergo severe plastic deformation and become nanostructured during ball milling. It is well established that formation of nano-crystalline material is accompanied with an enhancement in the diffusion rate in the nonequilibrium grains, a reduction in the diffusion distance, an extension in the solid solubility and, possibly, a depression in the melting point [15, 20, 34], that leads to creation of superior properties such as higher hardness.

4. Conclusion

The following conclusions have been drawn from this investigation:

1. The crystallite size of the WC powders decreased to less than 20 nm after 25 hours of milling and the internal strain increased to about 1.1 %percent.
2. The optimized sintering temperature was measured at 1350°C.
3. The 25-hours-milled powder exhibited significant densification on liquid phase sintering at 1350°C. So, the relative density of 98.2%TD was achieved.
4. At a constant sintering temperature (1350°C), the highest relative density (98.2%) and hardness (1281 HV30) were achieved for sample after 25h of milling.

Acknowledgements

The authors are grateful for support of this research by Isfahan University of Technology.

References

1. B. V. Desai, K. P. Desai, H. K. Raval, “Die-Less rapid prototyping process: Parametric investigations”, Procedia Materials Science, Vol. 6, 2014, pp. 666-673.
2. S. A. Hewitt, K. A. Kibble, “Effects of ball milling time on the synthesis and consolidation of nanostructured WC–Co composites”, Int. J. Refract. Met. Hard. Mater., Vol. 27, 2009, pp. 937–48.
3. Y. Wang, Z. Xu, “Nanostructured Ni–WC–

Co composite coatings Fabricated by electrophoretic deposition", Surf. Coat. Tech., Vol. 200, 2006, pp. 3896 –902.
4. G. Gille, J. Bredthauer., B. Gries, B. Mende, and W. Heinrich, "Advanced and new grades of WC and binder powder-their properties and application", Int. J. Refract. Met. Hard. Mater., Vol. 18, 2000, pp. 87–102.
5. K. P. Plucknet, P. F. Becher and K. B. Alexander, "In situ SEM observation of the fracture behaviour of Titanium Carbide/Nickel Aluminide composites", J. Microscopy, Vol. 185, 1997, pp. 206-216.
6. C. Hanyaloglu, B. Aksakal, J. D. Bolton, "Production and indentation analysis of WC/Fe-Mn as an alternative to cobalt-bonded hardmetals Materials Characterization", Vol. 47, 2001, pp. 315-322.
7. R. González, J. Echeberría, J. M. Sánchez and F. Castro, "WC-(Fe,Ni,C) hardmetals with improved toughness through isothermal heat treatments", J. Mater. Sci., Vol. 30(13), 1995, pp. 3435-3439.
8. J. M. Guilemany, I. Sanchiz, B. G. Mellor, N. Llorca, and J. R. Miguel, "Mechanical-Property Relationships of Co/WC and Co-Ni-Fe/WC Hard Metal Alloys", Int. J. Refract. Met. Hard. Mater., Vol. 12, 1993, pp. 199-206.
9. R. Cooper, S. A. Manktelow, F. Wong, L. E. Collins, "The sintering characteristics and properties of hard metal with Ni–Cr binders", Mater. Sci. Eng. A, Vol. 105-106, 1988, pp. 269-273.
10. T. W. Penrise, "Alternative binders for hard metals", J. Mater. Shap. Tech., Vol. 5, 1987, pp. 35-9.
11. V. A. Tracey, "Nickel in hardmetals", Int. J. Refract. Met. Hard. Mater., Vol. 11, 1992, pp. 137-149.
12. L. Prakash, Proceedings of 12th International Plansee Seminar, Reutte, H. Bildstein, ed., Pion Ltd, London, UK, 1990.
13. B. Wittmann, W.D.Schubert, B. Lux, "WC grain growth and grain growth inhibition in nickel and iron binder hardmetals". Int. J. Refract. Met. Hard. Mater., Vol. 20, 2002, pp. 51–60.
14. *C. T. Peters and S. M. Brabyn***, "***Properties of nickel substituted* hardmetals and their performance in hard rock drill bits". Met. Powd. Rep., Vol. 42, 1987, pp. 863–865.
15. F. L. Zhang, C. Y. Wang, M. Zhu, "Nanostructured WC/Co copmposite powder prepared by high energy ball milling", Scripta. Mater., Vol. 49, 2003, pp. 1123-28.
16. M. S. El-Eskandarany, A. A. Mahday, H. A. Ahmed, A. H. Amer, "Synthesis and characterizations of ball-milled nanocrstalline WC and nanocomposite WC-Co powders and subsequent consolidations", J. Alloy. Compd., Vol. 312(1-2), 2000, pp. 315-25.
17. Z. Zak Fang, Xu Wang, T. Ryu, K. Sup Hwang, H.Y. Sohn, "Syntesis, sintering, and mechanical properties of nanocrystalline cemented tungsten carbide-A review", Int. J. Refract. Met. Hard. Mater., Vol. 27, 2009, pp. 288-299.
18. G. K. Williamson, W. H. Hall, "X-ray Line Broadening from Filed Aluminium and Wolfram", Acta. Metall., Vol. 1, 1953, pp. 22-31.
19. Y. D. Kim, J. Y. Chung, J. Kim, H. Jeon, "Formation of nanocrystalline Fe–Co powders produced by mechanical alloying", Mater. Sci. Eng., Vol A291, 2000, pp. 17-21.
20. H. Moumenia, S. Alleg, J. M. Greneche, "Structural properties of $Fe_{50}Co_{50}$ nanostructured powder prepared by mechanical alloying", J. Alloy. Compd, Vol. 386, 2005, pp. 12–19.
21. C. Suryanarayana, "Mechanical alloying and milling", Prog. Mater. Sci., Vol. 46, 2001, pp. 1-184.
22. Y. Zhong, L. L. Shaw, "Growth mechanisms of WC in WC–5.75 wt% Co". Ceram. Int., Vol. 37, 2011, pp. 3591–3597.
23. Upadhyaya, G. S., "Cemented Tungsten Carbides: Production, Properties and Testing", Noyes Publication, 1998.
24. A. V. Shatov, S. A. Firstov, I. V. Shatova, "The shape of WC crystals in cemented carbides", Mater. Sci. Eng.A, Vol. 242, 1998, pp. 7–14.
25. I. J. Shon, I. K. Jeong., I. Y. Ko, J. M. Doh, K. D. Woo, "Sintering behavior and mechanical properties of WC–10Co, WC–10Ni and WC–10Fe hard materials

produced by high-frequency induction heated sintering", Ceram. Int., Vol. 35, 2009, pp. 339–344.
26. S. Kim, S. H. Han, J. K. Park, H. E. Kim, "Variation of WC grain shape with carbon content in the WC–Co alloys during liquid-phase sintering", Scrip. Mater., Vol. 48, 2003, pp. 635–639.
27. S. J. L. Kang, "Sintering: Densification, Grain Growth, and Microstructure", Elsevier Butterworth-Heinemann Linacre House, Jordan Hill, Oxford OX2 8DP, 2005.
28. C. S. Kim, T. R. Massa, G. S. Rohrer, "Modeling the relationship between microstructural features and the strength of WC–Co composites", Int. J. Refract. Met. Hard. Mater., Vol. 24, 2006, pp.89–100.
29. H. C. Lee, J. Gurland, "Hardness and deformation of cemented tungsten carbides", Mater. Sci. Eng., Vol. 33, 1978, pp. 125-133.
30. S. Cha, K. Lee, H. Ryu, S. Hong, "Analytical modeling to calculate the hardness of ultra-fine WC-Co cemented carbides", Mater. Sci. Eng., Vol. A489, 2008, pp. 234-44.
31. M. A. Xueming, J. I. Gang, Z. Ling, D. Yuanda, "Structure and properties of bulk nano-structured WC–CO alloy by mechanical alloying", J. Alloy. Compd., Vol. 264, 1998, pp. 267–270.
32. A. V. Shatov, S. S. Ponomarev, S. A. Firstov, "Modeling the effect of flatter shape of WC crystals on the hardness of WC-Ni cemented carbides", Int. J. Refract. Met. Hard. Mater., Vol. 27, 2009, pp. 198–212.
33. A. Delanoe, S. Lay, "Evolution of the WC grain shape in WC–Co alloys during sintering: Effect of C content", Int. J. Refract. Met. Hard. Mater., Vol. 27, 2009, pp. 140–148.
34. M. H. Enayati, G. R. Aryanpour., A. Ebnonnasir, "Production of nanostructured WC-Co powder by ball milling", Int. J. Refract. Met. Hard. Mater., Vol. 27, 2009, pp. 159-163.
35. F. L. Zhang, M. Zhu and C. Y. Wang, "Parameters optimization in the planetary ball milling of nanostructured tungsten carbide/cobalt powder", Int. J. Refract. Met. Hard. Mater., Vol. 26, 2008, pp. 329-333.